

**Laser Based Angle-Resolved Photoemission
Spectroscopy and High T_c Superconductivity**

by

Jacob D. Koralek

B.S., University of California Santa Barbara, 1999

M.S., University of Colorado, 2004

A thesis submitted to the
Faculty of the Graduate School of the
University of Colorado in partial fulfillment
of the requirements for the degree of
Doctor of Philosophy
Department of Physics
2006

This thesis entitled:
Laser Based Angle-Resolved Photoemission Spectroscopy and High T_c
Superconductivity
written by Jacob D. Koralek
has been approved for the Department of Physics

Daniel S. Dessau

Steven T. Cundiff

Date _____

The final copy of this thesis has been examined by the signatories, and we find that both the content and the form meet acceptable presentation standards of scholarly work in the above mentioned discipline.

Koralek, Jacob D. (Ph.D., Physics)

Laser Based Angle-Resolved Photoemission Spectroscopy and High T_c Superconductivity

Thesis directed by Prof. Daniel S. Dessau

A laser based system for performing high resolution angle-resolved photoemission spectroscopy (ARPES) is presented. This system uses 6 eV photons from the fourth harmonic of a Ti:Sapphire oscillator, which increases the bulk-sensitivity of ARPES by about an order of magnitude compared to higher energy synchrotron based sources. The laser system also offers an order of magnitude improvement in both photon flux and momentum resolution. The greatly reduced operating costs of the laser ARPES system should make the ARPES technique available to researches without access to synchrotron light sources. The details of the design, construction, and calibration of all aspects of the laser ARPES system are all discussed in this thesis.

Laser ARPES is used to study the high T_c superconductor $\text{Bi}_2\text{Sr}_2\text{CaCu}_2\text{O}_{8+\delta}$ (Bi2212), which is perhaps the material most heavily studied with ARPES. These low energy ARPES experiments are found to be in the sudden limit for states near the Fermi surface, accurately reproducing the qualitative features seen in previous studies of this material. The improvements in resolution have facilitated the first observation of spectral peaks which are sharp on the scale of their energy - the clearest evidence yet for quasiparticles in the normal state of a high T_c superconductor. This brings ARPES measurements of the quasiparticle scattering rate into agreement with optical transport measurements for the first time. The width of these peaks in momentum space corresponds to a nodal mean free path far greater than the length scale of the gap inhomogeneity seen in scanning tunneling

microscopy (STM) measurements.

The peak-dip-hump lineshape is introduced to fit the emergence of a high energy spectral hump in underdoped Bi2212. A very high resolution study of the superconducting gap symmetry is presented, revealing significant contributions to the gap from higher order d -wave harmonics in agreement with previous studies. This feature of the gap symmetry is found to likely be intrinsic to the pairing interaction, indicating an interaction range beyond nearest-neighbor lattice sites.

A linear temperature dependence to the nodal Fermi velocity is observed at all doping levels, possibly indicating a new many-body effect. Simulations of the coupling of electrons to various collective excitations indicate the qualitative requirements of the bosonic spectrum: it must contain a sharp spike in order to produce the dispersion kink, but must also possess a component which extends over a broad energy range in order to produce the linear temperature dependence of the Fermi velocity.

Above all else, the work presented here paves the way for the use of lasers as an ARPES light source. The improvements offered by this new technique, as well as the possibility to do time-resolved pump-probe ARPES, indicate a promising future for lasers in the direct study of electronic interactions in solids.

Dedication

To my family.

Acknowledgements

First of and foremost I would like to thank my parents. They have encouraged and supported me throughout all stages of my education, and for that I am forever grateful.

My advisor Dan Dessau has been an exceptional mentor and friend. He entrusted me with a very ambitious project, and supplied me with all of the support necessary to succeed. Steve Cundiff, Henry Kapteyn and Margaret Murnane have really been like co-advisors to me. They have helped both me and Dan learn the optics required to develop the laser ARPES system. They have also been very generous in allowing to use their lab space and equipment, and have even helped pay for my salary and tuition (a very important part of the business).

A project of this magnitude would not have been possible without the strong group of students we have in the Dessau lab. When I joined the group, I learned from Adam Gromko, Yi-De Chuang, Alexei Fedorov and Phil Villella. Special thanks is due to Fraser Douglas who has devoted an enormous amount of time and effort working with me on this project. Zhe Sun, Nick Plumb, Qiang Wang, Justin Griffith and Ted Reber have all been essential in the success of this project, each with unique contributions.

Sample growth is an essential aspect of our research, which is often overlooked. Our high quality single-crystal samples were provided by Y. Aaira, Hiroshi Eisaki, Yoichi Ando, K. Oka, Lou Lombardo and Aharon Kapitulnik.

One of my biggest inspiration for pursuing graduate studies in physics came from my work in the lab of David Awschalom as an undergrad at UCSB. The graduate students that worked with me there, Jay Gupta, Darron Young and Scott Crooker, were the people who showed me how much fun experimental physics can be.

Others who have helped me out along the way (in no particular order): Chuck Rogers, Carl Lineberger, Erez Gershgoren, Tara Fortier, David Alchenberger, Ron Goldfarb, Tracey Buxkemper, Charley Bowen, Sid Gustafson, Hans Green, Eric Erdos, Kendall Reed, Paul Beckingham, Dan Sheehy, Doug Scalapino, Andrea Damascelli, George Sawatsky, Elihu Abrahams, Andrey Chubukov, Kieth Geller, Francesc Roig, Roger Freedman, and Jim Shepard.

Last but not least I thank Annalisa Schilla, the love of my life, and the best friend I have ever had. I just don't know what I would do without you.

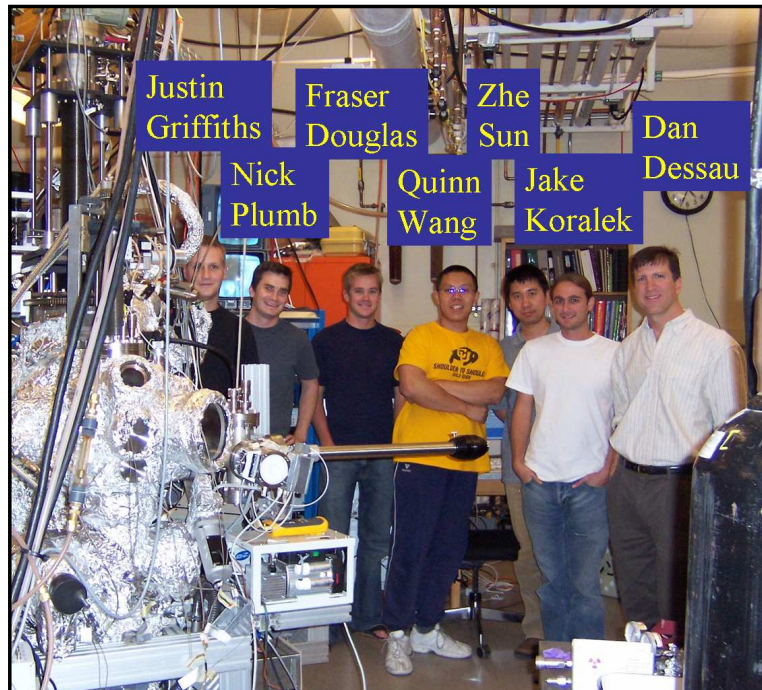


Figure 1: (color) The most complete Dessau group photo we have (2006).

Contents

Chapter		
1	Introduction	1
2	The Photoemission Technique	6
	2.1 Introduction	6
	2.2 Angle-integrated photoemission	7
	2.3 Angle-resolved photoemission	9
	2.4 Photoemission theory	11
	2.4.1 The three-step model	11
	2.4.2 The sudden approximation and spectral function	13
	2.4.3 The self-energy	14
	2.5 Energy and momentum distribution curves	17
3	Laser-Based ARPES	19
	3.1 Introduction	19
	3.2 Advantages of 6 eV laser ARPES	21
	3.2.1 Bulk sensitivity	22
	3.2.2 Momentum resolution	25
	3.2.3 Inelastic background	26
	3.3 The 6 eV photon source	28
	3.4 The analysis chamber	33

3.5	The electron spectrometer	36
3.5.1	Angular calibration	39
3.6	Data acquisition and system control software	43
3.7	Sample preparation for low-energy ARPES	45
3.8	Summary	46
4	Review of Superconductivity	47
4.1	Introduction	47
4.2	BCS superconductivity	51
4.3	High T_c superconductivity	57
4.3.1	Crystal structure	57
4.3.2	Doping phase diagram	59
4.3.3	d -wave superconductivity	61
4.3.4	Coupling of near-Fermi electrons to collective excitations	62
5	Sample Surface Ageing	65
5.1	Introduction	65
5.2	Experimental	65
5.3	XPS and laser ARPES	66
6	Laser ARPES Study of Optimally Doped Bi2212	71
6.1	Introduction	71
6.2	Experimental	72
6.3	The sudden approximation: comparison of laser and synchrotron based ARPES	74
6.4	Kramers-Kronig consistency of laser ARPES	82
6.4.1	Introduction	82
6.4.2	Application of Kramers-Kronig transformations to ARPES	82

6.5	Comparison to optics	87
6.6	Nodal mean free path	90
6.7	Lorentzian EDC fitting and nodal quasiparticles	92
6.7.1	Details of the EDC fitting procedure	92
6.7.2	Lorentzian EDC fitting results	96
6.8	Fermi liquid and marginal Fermi liquid EDC fitting	103
6.8.1	Fermi liquid fitting	103
6.8.2	Marginal Fermi liquid fitting	106
6.9	Summary of EDC fitting	109
6.10	Summary	111
7	Laser ARPES Study of Underdoped Bi2212	112
7.1	Introduction	112
7.2	Experimental	112
7.3	Doping dependence of lifetimes and mean free paths	113
7.4	Lorentzian EDC fitting	114
7.4.1	Single peak fitting	114
7.4.2	Double peak fitting	117
7.5	Superconducting gap symmetry	121
7.6	Summary	129
8	Temperature Dependence of the Nodal Fermi Velocity in Bi2212	130
8.1	Introduction	130
8.2	Experimental	132
8.3	Temperature dependent nodal Fermi velocity in Bi2212	133
8.4	Simulations of the electron-boson coupling	137
8.5	Summary	141

9	Summary and Future Directions	143
	Bibliography	147
	Author Index	156
	Appendix	
A	Abbreviations Used in this Thesis	163
B	Kramers-Kronig Program Code	165
C	CAD Renderings of the Laser ARPES Chamber	167
D	Angular Calibration Device 2 Technical Drawings	170

Tables

Table

6.1 Summary of χ^2 for different EDC fitting lineshapes 109

Figures

Figure

1	Dessau group photo (2006)	vii
2.1	Angle-integrated photoemission	8
2.2	Conservation of momentum	9
2.3	Angle-resolved photoemission	10
2.4	Idealized ARPES spectra for non-interacting and correlated systems	16
2.5	Energy and momentum distribution curves	18
3.1	Layout of a typical synchrotron ARPES beamline	20
3.2	The universal curve for surface sensitivity in photoemission	23
3.3	Calculated mean free path in Bi2212	24
3.4	The momentum space range of 6 eV ARPES in the 1 st Brillouin zone of Bi2212	27
3.5	The 6 eV laser system	29
3.6	Grenouille measurement of the output of the Ti:Sapphire oscillator	30
3.7	Fourth harmonic spectrum	31
3.8	Flux of undulator beamline 12.0.1 at the Advanced Light Source compared with the 6 eV laser	32
3.9	CAD drawings of the laser ARPES chamber	34
3.10	The laser ARPES lab	35

3.11	The Scienta electron spectrometer	37
3.12	Polycrystalline gold spectrum	38
3.13	Angular calibration device 1	39
3.14	Angular calibration device 2	41
3.15	ARPES calibration image	42
3.16	CU-ARPES screenshot	44
3.17	Photographs of a cleaved Bi2212 sample	46
4.1	Timeline of major advances in superconductivity	50
4.2	Spectral properties of a BCS superconductor	55
4.3	Crystal structure of the BSCCO family of cuprate superconductors	58
4.4	Generic doping phase diagram for cuprates	60
4.5	Anisotropy of the superconducting gap	61
4.6	Electronic structure effects from coupling of electrons to collective modes	63
4.7	Anti-nodal dispersion kink in Bi2212	64
5.1	XPS spectra from vacuum-cleaved Bi2212	67
5.2	Time dependence of the O 1s peaks I	69
5.3	Time dependence of the O 1s peaks II	70
6.1	Comparison of nodal dispersion, \mathbf{k} -scaled using different sample work functions	75
6.2	Nodal Fermi surface crossings	76
6.3	Comparison nodal ARPES spectra in optimally doped Bi2212 . .	78
6.4	Nodal MDC widths in optimal Bi2212	80
6.5	Superconducting gap in optimally doped Bi2212	81
6.6	Extraction of the self-energy from ARPES data	83

6.7	Kramer-Kronig consistency of laser ARPES data	86
6.8	Comparison of scattering rates from optics and laser ARPES . . .	89
6.9	Nodal mean free path at the Fermi surface from laser ARPES . .	91
6.10	EDC fitting background	94
6.11	Comparison of background lineshapes	95
6.12	Nodal ARPES data from optimally doped Bi2212 at different tem- peratures	97
6.13	Lorentzian EDC fits at several temperatures	98
6.14	Scattering rate in optimally doped Bi2212	99
6.15	Comparison of EDCs peaks away from the Fermi energy	102
6.16	Fermi liquid EDC fitting	105
6.17	Temperature dependence of $\text{Im}\Sigma$ at fixed energies	107
6.18	Fermi liquid and Marginal Fermi liquid fits compared	108
6.19	Residuals from EDC fitting	110
7.1	Doping dependence of EDCs and MDCs	113
7.2	Single Lorentzian EDC fitting	115
7.3	Scattering rate in underdoped Bi2212	116
7.4	Components of the peak-dip-hump fit	118
7.5	Nodal and off-nodal images with peak and hump dispersion	119
7.6	Scattering rate from peak-dip-hump fits	120
7.7	Superconducting gap symmetry for different doping levels	122
7.8	Momentum dependence of laser ARPES images in the supercon- ducting state	123
7.9	Location of gap data in the first Brillouin zone	123
7.10	EDCs at \mathbf{k}_F , at different points around the Fermi surface	125

7.11	Momentum dependence of the superconducting gap in underdoped Bi2212	127
7.12	Gap symmetry in the absence of the gapless region	128
8.1	Simulation of resolution effects in ARPES	131
8.2	Temperature dependence of the nodal dispersion in optimally doped Bi2212	134
8.3	Temperature dependence of the nodal Fermi velocity	135
8.4	Temperature dependence of $\text{Re}\Sigma^{\text{op}}$ in optimally doped Bi2212 from FTIR	136
8.5	Simulation of coupling to an Einstein phonon	138
8.6	The spectrum α^2F for the coupling of electrons to spin fluctuations	139
8.7	Simulation of coupling to spin fluctuations	140
C.1	CAD rendering 1 of the laser ARPES chamber	168
C.2	CAD rendering 2 of the laser ARPES chamber	169
D.1	Technical drawing of angular calibration device 2	170